

See discussions, stats, and author profiles for this publication at: <https://www.researchgate.net/publication/260716619>

How Viscoelastic Solution of Wormlike Micelles Transforms into Microemulsion upon Absorption of Hydrocarbon: A New Insight.

ARTICLE *in* LANGMUIR · MARCH 2014

Impact Factor: 4.46 · DOI: 10.1021/la500484e · Source: PubMed

CITATIONS

7

READS

76

7 AUTHORS, INCLUDING:



[Andrey Shibaev](#)

Lomonosov Moscow State University

2 PUBLICATIONS 7 CITATIONS

SEE PROFILE



[Vyacheslav Molchanov](#)

Lomonosov Moscow State University

14 PUBLICATIONS 135 CITATIONS

SEE PROFILE



[O. E. Philippova](#)

Lomonosov Moscow State University

82 PUBLICATIONS 1,419 CITATIONS

SEE PROFILE

How a Viscoelastic Solution of Wormlike Micelles Transforms into a Microemulsion upon Absorption of Hydrocarbon: New Insight

Andrey V. Shibaev,[†] Mikhail V. Tamm,^{†,‡} Vyacheslav S. Molchanov,[†] Andrey V. Rogachev,^{‡,§} Alexander I. Kuklin,^{‡,§} Elena E. Dormidontova,^{||} and Olga E. Philippova^{*,†}

[†]Physics Department, Moscow State University, 119991 Moscow, Russia

[#]Department of Applied Mathematics, National Research University Higher School of Economics, 101000 Moscow, Russia

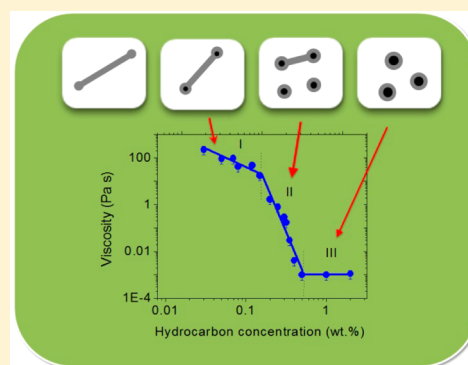
[‡]Joint Institute for Nuclear Research, 141980 Dubna, Russia

[§]Moscow Institute of Physics and Technology, 141700 Dolgoprudny, Russia

^{||}Institute of Materials Science and Physics Department, University of Connecticut, Storrs, Connecticut 06269, United States

S Supporting Information

ABSTRACT: In this article, we investigate the effect of hydrocarbon addition on the rheological properties and structure of wormlike micellar solutions of potassium oleate. We show that a viscoelastic solution of entangled micellar chains is extremely responsive to hydrocarbons—the addition of only 0.5 wt % *n*-dodecane results in a drastic drop in viscosity by up to 5 orders of magnitude, which is due to the complete disruption of micelles and the formation of microemulsion droplets. We study the whole range of the transition of wormlike micelles into microemulsion droplets and discover that it can be divided into three regions: (i) in the first region, the solutions retain a high viscosity ($\sim 10\text{--}350\text{ Pa}\cdot\text{s}$), the micelles are entangled but their length is reduced by the solubilization of hydrocarbons; (ii) in the second region, the system transitions to the unentangled regime and the viscosity sharply decreases as a result of further micelle shortening and the appearance of microemulsion droplets; (iii) in the third region, the viscosity is low ($\sim 0.001\text{ Pa}\cdot\text{s}$) and only microemulsion droplets remain in the solution. The experimental studies were accompanied by theoretical considerations, which allowed us to reveal for the first time that (i) one of the leading mechanisms of micelle shortening is the preferential accumulation of the solubilized hydrocarbon in the spherical end caps of wormlike micelles, which makes the end caps thermodynamically more favorable; (ii) the onset of the sharp drop in viscosity is correlated with the crossover from the entangled to unentangled regime of the wormlike micellar solution taking place upon the shortening of micellar chains; and (iii) in the unentangled regime short cylindrical micelles coexist with microemulsion droplets.



INTRODUCTION

Semidilute aqueous solutions of viscoelastic surfactants possess remarkable rheological properties owing to the formation of a transient network of very long entangled wormlike micelles (micellar chains). Even at rather low concentrations (a few wt %), such solutions can exhibit extremely high relative viscosities^{1,2} ($\sim 10^7$) and gel-like behavior,^{2,3} and in some cases they display an apparent yield stress.⁴ The rheological behavior of viscoelastic surfactants can be described by living polymer models taking into account the breakage and recombination of the micelles.^{5–7} Because of the self-healing ability of living micellar chains, their solutions have a significant advantage over similar polymeric systems because their mechanical degradation at high shear rates is completely reversible.

The unique rheological properties of viscoelastic surfactants are widely exploited commercially, for example, for drag reduction in heating/cooling systems,⁸ for viscosity modification in consumer products (bleach, liquid dishwashing

detergents, and cosmetics), and in various fluids used in oil recovery.^{9–11} In many of these applications (e.g., in cosmetics and enhanced oil recovery), the micelles come into contact with nonpolar substances, which can be easily solubilized inside the micellar cores, thus affecting the structure of the micelles and therefore the rheological properties.

There are many papers describing the effect of the encapsulation of small amounts of hydrocarbons on the rheology of wormlike micellar solutions.^{12–19} They show that the rheological behavior of such systems is strongly related to the site of oil location within the hydrophobic core of micelles (deep inside the core or closer to the surface). For example, solubilization in the interior part of the core (as in the case of strongly hydrophobic long-chain *n*-alkanes) leads to a decrease in viscosity.^{14,17} By contrast, solubilization at or near the core/

Received: February 6, 2014

Revised: March 11, 2014

Published: March 11, 2014

water interface (as in the case of benzene in cationic surfactant micelles) increases the viscosity.¹³ The increase in viscosity is explained by the elongation of micelles (without any change in their radii) as a result of lowering both the electrostatic repulsion between headgroups and the hydrocarbon/water contact free energy.^{12,20} However, when the outer layer becomes saturated with hydrocarbon, additional hydrocarbon penetrates the core deeply, leading to a decrease in viscosity.¹³

Therefore, independently of the initial site of solubilization, at later stages hydrocarbon is encapsulated in the inner part of the core, and the viscosity diminishes. The decrease in viscosity was explained by the shortening of micelles with simultaneous radial growth.^{14,17,21} For instance, in ref 14 it was demonstrated that the 20-fold decrease in the viscosity of an aqueous solution of erucyl bis(hydroxyethyl) methylammonium chloride upon absorption of hexane is accompanied by a 10-fold shortening of micelles related to a slight lowering of the scission energy of micellar chains from 81 ± 8 to 72 ± 7 kJ/mol. However, the reasons for the shortening of micelles are still poorly understood. In ref 17, the authors suggest that oil solubilized in the core increases the interfacial curvature of micelles and stabilizes the end caps, thus favoring the formation of shorter micelles. But this explanation seems not to be very clear because the growing volume of the core as a result of the absorption of oil should reduce the interfacial curvature rather than increase it. Thus, the current understanding of the change in micellar length induced by hydrocarbon addition relies on the fact that hydrocarbon is solubilized in the cylindrical body of the micelle, changing its radius and curvature and therefore its length. However, if long wormlike micelles are formed in the solution, the packing of surfactant molecules in the cylindrical body is optimal, and even its small change would be very disadvantageous. However, the hemispherical end caps of cylindrical micelles are thermodynamically unfavorable, and it would be much more effective for hydrocarbons to be solubilized in the end caps, making their curvature closer to optimal. As far as we know, until now only the location of oil either deep in the core or in the palisade region of wormlike micelles has been discussed, whereas the possibility of the more efficient accumulation of oil in end caps in comparison to the cylindrical part of micellar chains has not been considered.

Several papers^{22–25} have addressed the situation in which excess hydrocarbon is added to wormlike micelles. In this case, the encapsulated hydrocarbon completely destroys the micellar chains, yielding microemulsion droplets and a very low solution viscosity.

Thus, until now the impact of absorbed hydrocarbon on the rheology of wormlike micellar solutions was mainly studied for two extreme cases: for very small amounts of added oil, giving oil-containing worms, and for large amounts of added oil, providing microemulsion droplets. At the same time, there are only a few papers^{17,22,26} describing the whole range of transition from wormlike micelles to microemulsion droplets. In ref 22, it was shown that the addition of oil to perfluorinated surfactants induces a 4 order of magnitude drop in viscosity. It was noted that the lowering of viscosity is accompanied by a decrease in the shear modulus and the structural relaxation time. The authors attribute this behavior to the increase in the radius of wormlike micelles, leading to the shortening of the total length of micelles and hence to the reduction of the number density of entanglement points. It was shown that as a result of the solubilization of a large amount of oil the network properties were lost.²² However, the rheological measurements

have not been supplemented by the structural characterization except for the extreme case, where only microemulsion droplets are present in the solution. It was surprisingly discovered that the radius of microemulsion droplets decreased with the addition of oil.²² For hydrogenated surfactants, the gradual addition of hydrocarbon to entangled cylindrical micelles has been studied by static and dynamic light scattering.²⁶ It has been shown that the light-scattering intensity decreases by up to 1 order of magnitude at a characteristic hydrocarbon concentration. This decrease was attributed to the transition from rodlike micelles to microemulsion droplets; however, it remained unclear whether this transition proceeds via the gradual shortening of micellar chains or through the coexistence of shortened micelles with microemulsion droplets.

As for theoretical studies, the thermodynamics and rheology of solutions of wormlike micelles have been extensively investigated,^{5–7,27–29} but there are only a few theoretical^{30,31} and computer simulation³² studies on the solubilization of hydrocarbons in micelles. In ref 32, the solubilization of oil droplets by spherical surfactant micelles has been modeled by molecular dynamics simulations. In ref 30, a theoretical model of the solubilization of hydrocarbons in spherical microemulsions and rodlike surfactant micelles has been discussed. In some cases, the transition from rodlike micelles to spheres with an increase in the solubilization ratio has been predicted. To the best of our knowledge, the interplay between the solubilization of hydrocarbons in wormlike micelles and the change in their structural properties has never been discussed in terms of the molecular mechanism of the transformation.

The aim of this article is to study simultaneously the rheological and structural changes that accompany the whole range of transition of wormlike micelles into microemulsion droplets induced by the absorption of hydrocarbon. To this end, we employ a combination of rheological measurements to study macroscopic properties (viscosity, elasticity, etc.), scattering techniques (small-angle neutron scattering (SANS) and dynamic light scattering (DLS)) to follow the structural changes occurring on the microscopic level, and analytical analysis to gain insight into the molecular mechanisms of wormlike micelle transformation. As a result of these studies, it is demonstrated that a small amount of hydrocarbon induces a dramatic drop in the viscosity of the system by 5 orders of magnitude. We identify and characterize different stages of the transition of wormlike micelles into microemulsion droplets and discuss the preferential mechanism of oil encapsulation. We show that the onset of the sharp drop in viscosity takes place at the crossover from the entangled to unentangled regime, which occurs upon shortening of the micelles. We demonstrate for the first time that the drop in viscosity upon addition of oil is due to both the shortening of micellar chains and the appearance of microemulsion droplets, which become dominant at larger oil content. The obtained insights into the structural changes responsible for the observed drastic decrease in viscosity contribute to the general understanding of the molecular mechanisms of oil encapsulation by surfactant micelles and have important implications for a range of practical applications, such as oil recovery.

■ EXPERIMENTAL SECTION

Materials. Potassium oleate was purchased from Aldrich as a 40 wt % paste in water. Its critical micelle concentration in water is $(7–14) \times 10^{-4}$ M.^{33,34} Potassium chloride (purity >99.8%) from Helicon, potassium hydroxide (purity >99%) from Riedel-de Haën, and *n*-

dodecane (purity >99%) from Merck were used as received. Solutions were prepared using distilled deionized water purified by a Millipore Milli-Q system. D₂O for SANS experiments (99.9% isotopic purity) was supplied by Merck.

Samples Preparation. Potassium oleate solutions were initially prepared without hydrocarbon by mixing the appropriate quantities of surfactant and salt solutions with distilled water. A constant value of pH 12.3 ± 0.1 was kept for all samples by adding potassium hydroxide. The samples were stirred using a magnetic stirrer and then left to equilibrate at room temperature for 3 to 4 days to obtain homogeneous solutions and remove air bubbles. After that, different amounts of *n*-dodecane were added, and the solutions were stirred again and then left to equilibrate for 2–4 days.

For small amounts of added hydrocarbon (less than 0.6 and 3 wt % of *n*-dodecane for the 1.5 and 3 wt % potassium oleate solutions, respectively), all of the solutions thus prepared were fully transparent and did not phase separate with time. For larger amounts of added hydrocarbon, a thin layer of the hydrocarbon-rich phase was formed at the top of the aqueous solution. In this article, we limited our studies to the range of small hydrocarbon concentration when no phase separation was observed.

Rheology. Rheological measurements were performed with a Haake Rheostress 150L stress-controlled rotational rheometer at 20 °C. A cone–plate measurement cell with 35 mm diameter and a 2° cone angle was used to examine the samples with high viscosities (>1 Pa·s). Less viscous samples were investigated using double-gap coaxial cylinders (cup of 20.28 mm diameter, bob of 18 mm diameter and 55 mm height). A vapor lock filled with solvent was used to prevent solvent evaporation. In steady shear (static) experiments, the shear stress was varied in the range of 0.005–10 Pa. The zero-shear viscosity was determined as the value of viscosity on the plateau at low stress. Oscillatory shear (dynamic) measurements were taken over the angular frequency ω range of 0.06–65 1/s.

Small-Angle Neutron Scattering. SANS experiments were performed with the two-detector YuMO instrument of the IBR-2 high-flux pulsed reactor at the Frank Laboratory of Neutron Physics, Joint Institute for Nuclear Research, Dubna, Russia. The data were recorded in the range of the scattering vector q of 0.006 – 0.5 \AA^{-1} . The details of the measurements are described elsewhere.^{24,35–37} In these experiments, the samples were put into specially constructed dismountable cells with parallel quartz plates and a beam path of 2 mm. D₂O was used as a solvent, whereas both surfactant and hydrocarbon were hydrogenated. The scattering-length densities estimated for the surfactant tails, hydrocarbon, and D₂O were equal to ca. -0.30×10^{-6} , -0.48×10^{-6} , and $6.36 \times 10^{-6} \text{ \AA}^{-2}$, respectively. Therefore, we assumed that the micelles with solubilized hydrocarbon had a rather uniform scattering length density distribution throughout their volume (relative to D₂O).

Experimental data for the solutions with 0 and 1 wt % hydrocarbon (containing only cylindrical micelles or only microemulsion droplets, respectively) were analyzed using the program FITTER.³⁸ Only one fitting parameter (cross-sectional radius of a cylindrical micelle or radius of a microemulsion droplet) was used. To fit the scattering curves of the solutions containing 0.30, 0.35, and 0.45 wt % hydrocarbon, the program MIXTURE³⁹ was applied. The scattering curves were fitted by a mixture of cylinders and spheres. For the solutions at 0.30 and 0.35 wt %, we used three fitting parameters (relative volume fraction of cylinders in the mixture, cross-sectional radius of a cylinder, and radius of a sphere). However, the change in the cylinder radius was restricted within the range of 10–30 Å (knowing that the value should be close to the length of the fully extended alkyl surfactant tail, 19 Å), and the sphere radius was varied in the range of 10–80 Å. The relative volume fractions of cylinders φ_{cyl} and spheres φ_{sph} in the mixture were related by the equation $\varphi_{\text{cyl}} + \varphi_{\text{sph}} = 1$. For the solution at 0.45 wt %, the sphere radius was fixed by matching the experimental and theoretical first Fourier maxima. In this case, two fitting parameters were used (volume fraction of cylinders and cylinder radius). Because the solutions were prepared at a rather high concentration of KCl (6 wt %), we assumed that the electrostatic

interactions are almost fully screened, which allowed us to neglect the interactions between objects.

Dynamic Light Scattering. DLS experiments were carried out with an ALV/DLS/SLS-5022F goniometer system with an ALV-6010/EPP digital time correlator (ALV, Langen, Germany), a helium–neon laser (wavelength 632.8 nm), and a computer-controlled, stepping-motor-driven variable-angle detection system. Prior to measurements, the samples were filtered through 0.22 \mu m polyvinylidene fluoride Millex-GV filters (Millipore). The details of the experiments are described elsewhere.^{40–42}

THEORETICAL SECTION

The packing of surfactant molecules in a cylindrical micelle is normally characterized by two parameters: the radius of the micelle b and the surface area per surfactant molecule a . These parameters satisfy two conditions: (i) $b < b_{\text{max}}$, where b_{max} is the contour length of the hydrocarbon tail of the surfactant molecule, and (ii) $\nu = ab/2 = \text{const}$, where ν is the excluded volume of the molecule, which can be assumed to be independent of the external conditions. (Note that a spherical micelle is characterized by similar parameters but under the condition $\nu = a_{\text{sph}}b/3$.)

The specific (per molecule) free energy of a micelle can be written⁴³ as a sum of surface and bulk contributions

$$\varepsilon = \varepsilon_{\text{surf}} + \varepsilon_{\text{bulk}} \quad (1)$$

which behave quite differently as functions of the surface area per molecule a . The surface contribution $\varepsilon_{\text{surf}}$ is the sum of a surface tension contribution, which grows (approximately linearly) with a , and head-to-head electrostatic repulsion, which decreases with a . The resulting energy has a minimum at a certain a_0 , and in the vicinity of this minimum, it can be approximated by

$$\varepsilon_{\text{surf}} = \gamma a \left(1 - \frac{a_0}{a} \right)^2 \quad (2)$$

where typical experimental values of γ are on the order of $\gamma \approx 0.12kT/\text{\AA}^2$. In turn, the bulk contribution $\varepsilon_{\text{bulk}}$ is essentially independent of b (and therefore a) if the chains are not elongated beyond their maximum length b_{max} and grows extremely fast when the limit $b = b_{\text{max}}$ is exceeded. Therefore, for most purposes one can write

$$\varepsilon_{\text{bulk}} = \begin{cases} \text{const,} & \text{if } b < b_{\text{max}}, a > \alpha\nu/b_{\text{max}} \\ \infty, & \text{if } b > b_{\text{max}}, a < \alpha\nu/b_{\text{max}} \end{cases} \quad (3)$$

where $\alpha = 2$ and 3 for cylindrical and spherical micelles, respectively. Thus, amphiphilic molecules of a given chemical structure tend to form micelles with an optimal area per molecule a_0 , provided that the condition $a_0 > \alpha\nu/b_{\text{max}}$ is satisfied. In particular, if $a_0 > 3\nu/b_{\text{max}}$, then they form spherical micelles (which are preferable for entropic reasons), whereas for cylindrical micelles one always has $3\nu/b_{\text{max}} > a_0 > 2\nu/b_{\text{max}}$.

Now, in the end caps of a cylindrical micelle, which have an approximately semispherical shape, the area per molecule has to be larger than the preferred one for cylindrical arrangement (indeed, its lower boundary is $3\nu/b_{\text{max}} > a_0$). This is exactly what makes the end caps unfavorable and leads to the micelles being extremely long. To estimate the energy cost δ of a single end cap, we write

$$\delta = Q\Delta\varepsilon \quad (4)$$

where Q is the number of molecules in the end cap, whereas $\Delta\epsilon$ is the typical excess energy per molecule. Because the optimal radius of the end cap obviously equals b_{\max} (a larger radius would lead to increase in ϵ_{surf} without any gain in ϵ_{bulk}), one can write the following estimates

$$a_{\text{sph}} = \frac{3\nu}{b_{\max}}; Q \approx \frac{2\pi b_{\max}^2}{a_{\text{sph}}} = \frac{2\pi b_{\max}^3}{3\nu} \quad (5)$$

where a_{sph} is the typical area per molecule in the end cap and

$$\Delta\epsilon = \epsilon_{\text{sph}} - \epsilon_{\text{cyl}} \approx \frac{\gamma(3\nu - a_0 b_{\max})^2}{3\nu b_{\max}} = \frac{\gamma(a_{\text{sph}} - a_0)^2}{a_{\text{sph}}} \quad (6)$$

One finally arrives at the following estimate for δ :

$$\delta \approx 2\pi\gamma b_{\max}^2 \left(1 - \frac{a_0}{a_{\text{sph}}}\right)^2 \quad (7)$$

This energy, which in most of the experimentally studied systems is on the order of tens kT , has the meaning of half the scission energy – to cut a micelle in half, one should form two new end caps, requiring energy 2δ . As a result, the average aggregation number of a micelle (or the average contour length L) is given by²⁷

$$\langle n \rangle \sim L \sim \sqrt{c} \exp(\delta/kT) \quad (8)$$

where c is the concentration of the surfactant molecules.

RESULTS AND DISCUSSION

The rheological properties of semidilute solutions of potassium oleate far above the overlap concentration ($C^* \approx 0.1$ wt %) were studied in the presence of different amounts of n -dodecane. The concentration of added low-molecular-weight salt KCl was fixed at 6 wt %, which ensured the formation of very long linear wormlike micellar chains.^{24,45} The presence of wormlike micelles in the initial solution of potassium oleate (before the addition of hydrocarbon) has been previously established by SANS studies.^{24,25} These long micellar chains are responsible for the high viscosity of the solutions that can reach ~ 350 Pa·s.

Figure 1 shows the dependence of the zero-shear viscosity of potassium oleate solutions on the concentration of added n -dodecane. As can be seen, the gradual addition of hydrocarbon results first in a slight decrease of viscosity (region I) and then a drastic drop (region II) to 10^{-3} Pa·s, after which the viscosity remains constant (region III). The overall decrease in viscosity can reach 4 to 5 orders of magnitude. As a result, a highly viscous solution is transformed into a liquid with the viscosity close to that of pure water (10^{-3} Pa·s). Such a dramatic effect is achieved upon addition of less than 0.5 wt % n -dodecane. The lower the concentration of surfactant, the smaller the amount of hydrocarbon needed to achieve a viscosity of 10^{-3} Pa·s (Figure 1).

In the region of high viscosity (region I), the system displays a well-defined plateau in the frequency dependence of the storage modulus $G'(\omega)$ (Figure 2a) indicating the presence of a network of entangled wormlike micelles.^{1,46,47} In region II, where a drastic drop in viscosity occurs, the surfactant solution loses its viscoelasticity: the plateau in the frequency dependence of G' disappears and the loss modulus G'' becomes greater than the storage modulus G' over almost all of the studied

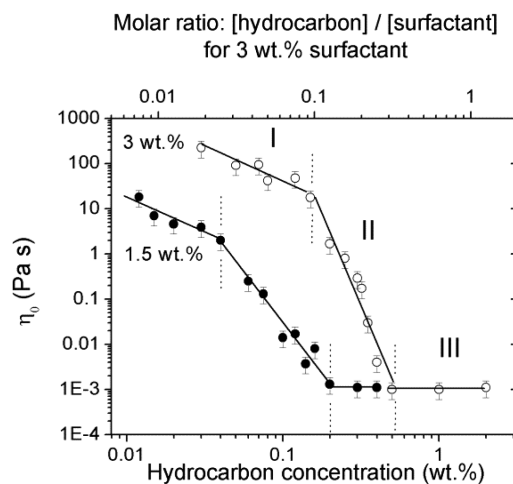


Figure 1. Zero-shear viscosity of 1.5 wt % (filled symbols) and 3 wt % (open symbols) potassium oleate solutions as a function of concentration of added n -dodecane. The upper axis shows the molar ratio $[n\text{-dodecane}]/[\text{potassium oleate}]$ for 3 wt % potassium oleate solution. Temperature: 20 °C. Solvent: 6 wt % KCl in water. Error bars are estimated on the basis of the results of repeated measurements.

frequency range (Figure 2a). At large concentrations of hydrocarbon (region III), the system always has a viscosity close to that of pure water, which is due to the formation of microemulsion droplets as has been evidenced by SANS.^{24,25}

Thus, the rheological behavior of potassium oleate solutions upon addition of n -dodecane can be subdivided into three regimes: (1) a micellar network regime, occurring at very low hydrocarbon concentrations, (2) a transition regime, where the viscosity drops by several orders of magnitude, and (3) the microemulsion regime, where viscosity remains close to that of pure water. We will discuss these regimes in more detail below.

Micellar Network Regime. In this regime, at very small hydrocarbon concentrations the frequency dependences of G' always show a wide plateau (Figure 2a), which for surfactant solutions is characteristic of a transient network of entangled wormlike micelles. The rheological behavior in this regime is well-described by a Maxwell model with a single relaxation time, as follows from the nearly semicircular shape of the Cole–Cole plot (Figure 2b). In wormlike micellar solutions, the Maxwell behavior is observed when the breaking time of the micellar chains is much shorter than the reptation time ($\tau_{\text{br}} \ll \tau_{\text{rep}}$).⁷ In such a fast-breaking limit, wormlike micelles break and recombine many times during reptation. This leads to the averaging of the relaxation processes, which therefore can be described by only one characteristic relaxation time τ . This relaxation time can be determined from the equation $\tau = 1/\omega_c$, where ω_c is the frequency at which G' and G'' intercept. The fact that at small concentrations of hydrocarbon the wormlike micelles are in the fast-breaking regime is also confirmed by the scaling dependences of the zero-shear viscosity η_0 and relaxation time τ on the concentration of surfactant (at a fixed surfactant/hydrocarbon molar ratio) (Figure 3), which match the theoretical predictions for the fast-breaking limit:^{5,6,47} $\eta_0 \sim c^{3.5}$ and $\tau \sim c^{1.25}$. The scaling exponent for the plateau shear modulus is found to be close to the theoretical predictions⁴⁷ for entangled wormlike micelles $G_0 \sim c^{2.25}$.

To understand the origin of the decrease in viscosity η_0 upon addition of hydrocarbon in this regime, the behavior of the

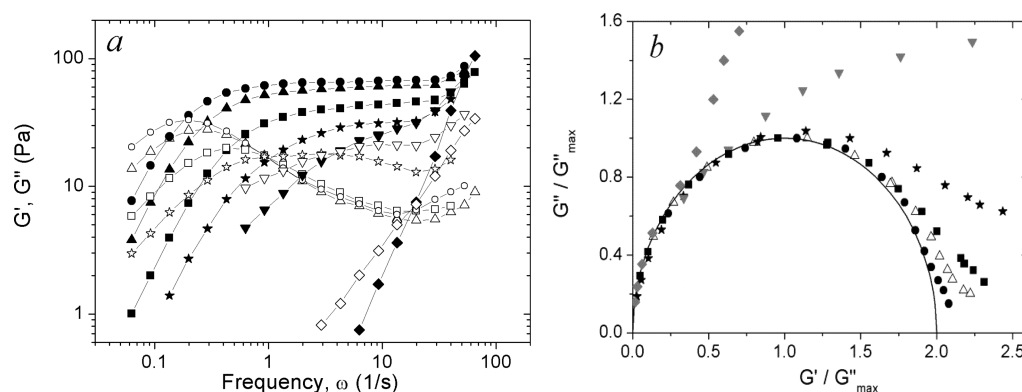


Figure 2. Frequency dependences of storage modulus G' (filled symbols) and loss modulus G'' (open symbols) (a) and Cole–Cole plot (b) for 3 wt % potassium oleate solutions at different concentrations of n -dodecane: 0 wt % (circles), 0.03 wt % (triangles), 0.07 wt % (squares), 0.15 wt % (stars), 0.25 wt % (reverse triangles), and 0.3 wt % (diamonds). Temperature: 20 °C. Solvent: 6 wt % KCl in water. The solid semicircle in the Cole–Cole plot represents the theoretical dependence calculated using the Maxwell model.

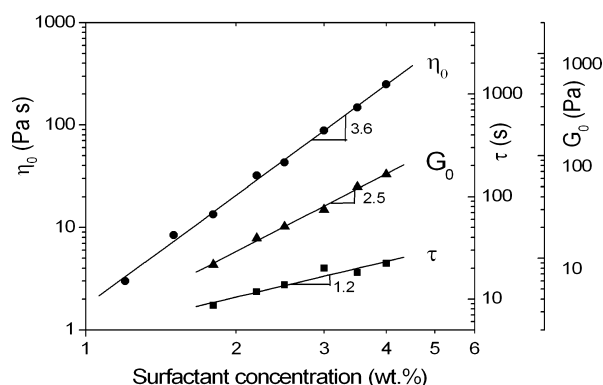


Figure 3. Dependences of zero-shear viscosity η_0 , relaxation time τ , and plateau shear modulus G_0 on potassium oleate concentration at fixed molar ratio $[n\text{-dodecane}]/[\text{potassium oleate}] = 1/50$. Temperature: 20 °C. Solvent: 6 wt % KCl in water.

plateau modulus G_0 and the relaxation time τ should be analyzed because for a Maxwell system the viscosity can be represented as the product of these values:⁴⁷ $\eta_0 = G_0\tau$. As seen from Figures 2a and 4, with the addition of n -dodecane both the plateau modulus G_0 and the relaxation time τ become smaller.

The plateau modulus G_0 decreases with hydrocarbon concentration c_h as $G_0 \sim c_h^{-0.42}$ (Figure 4). One of the reasons

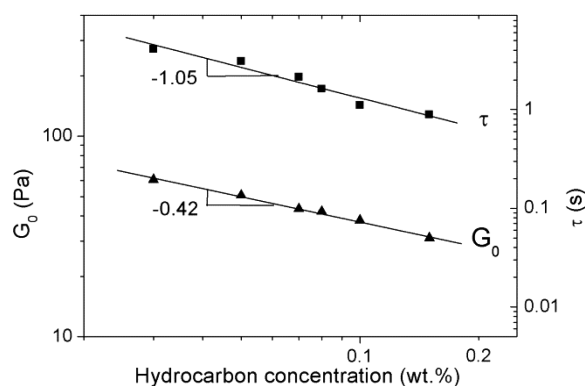


Figure 4. Dependences of plateau shear modulus G_0 and relaxation time τ on n -dodecane concentration for 3 wt % potassium oleate solutions. Temperature: 20 °C. Solvent: 6 wt % KCl in water.

for such behavior might be the increase in the rigidity of wormlike micelles when hydrocarbon is accumulated inside. Indeed, thicker rods are harder to bend than thinner ones. More rigid chains with a higher persistence length l_p should have a lower plateau modulus G_0 because⁷

$$G_0 \approx \frac{kT}{\xi^3} \approx \frac{kT}{l_e^{9/5} l_p^{6/5}} \quad (9)$$

where ξ is the mesh size of the network and l_e is the entanglement length. To test how the solubilization of hydrocarbon affects the micellar persistence length, SANS was used. (For details of the experiments, see the Supporting Information.) The results are presented in Table 1. It is seen

Table 1. Values of Persistence Length of Cylindrical Micelles l_p for 0.11 wt % Potassium Oleate Solutions with Different Concentrations of Added n -Dodecane Extracted from SANS Data

concentration of n -dodecane, wt %	molar ratio $[n\text{-dodecane}]/[\text{potassium oleate}]$	l_p , Å
0	0	173 ± 7
0.00073	1/80	181 ± 8
0.00183	1/32	190 ± 8
0.00330	1/18	188 ± 8

that l_p increases only slightly when the molar ratio $[n\text{-dodecane}]/[\text{potassium oleate}]$ is changed from 0 to 1/18. This small growth of l_p cannot account for the observed decrease in G_0 by nearly 40% (Figure 4).

Another reason for the lowering of G_0 may be connected to the increase in l_e resulting from the shortening of micellar chains. Indeed, the micelles have a rather wide length distribution, and if some of them that have $L \approx l_e$ become shorter, then they will no longer contribute to the elasticity.⁴⁸

The change in the average contour length L relative to l_e was estimated directly from the rheological data using the equation⁷

$$\frac{L}{l_e} \approx \frac{G_0}{G''_{\min}} \quad (10)$$

where G''_{\min} is the value of the loss modulus at the high-frequency minimum. The results are shown in Figure 5. As can be seen, the ratio of the average contour length of the micelles to the entanglement length decreases upon addition of

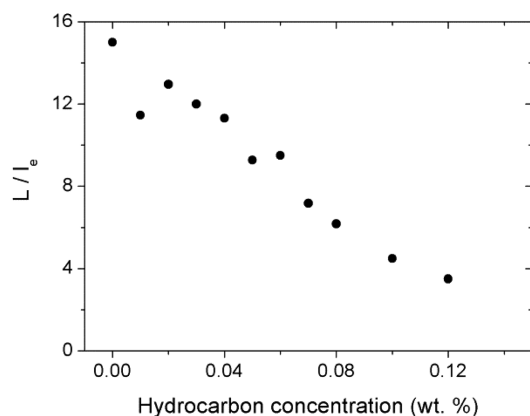


Figure 5. Dependence of the ratio of the average contour length of micelles L to entanglement length l_e on n -dodecane concentration for 3 wt % potassium oleate solutions. Temperature: 20 °C. Solvent: 6 wt % KCl in water.

hydrocarbon, approaching the limit $L \approx l_e$ at an oil content of about 0.15 wt % for 3 wt % potassium oleate solutions. Above this concentration of hydrocarbon, wormlike micelles are too short to be entangled and the solution loses its elasticity, as indicated by the disappearance of the elastic plateau in Figure 2a. Under these conditions ($L \approx l_e$), the crossover to region II occurs.

A decrease in G_0 was previously observed for wormlike micelles formed by mixed nonionic fluorinated surfactants upon absorption of perfluorodecalin.¹⁷ At the same time, for cationic surfactant erucyl bis(hydroxyethyl) methylammonium chloride no change in G_0 upon addition of up to 0.8 wt % n -hexane was detected.¹⁴ The difference in the observed behavior is possibly due to the solubilization of short n -alkanes (up to ca. C8) close to the headgroup region (in addition to the interior of the hydrocarbon core), which makes a shortening of the micelles and an increase in their radii less-pronounced.^{26,49}

As shown in Figure 4, the relaxation time τ decreases with the concentration of n -dodecane as $\tau \sim c_h^{-1}$. This behavior can be explained by the reduction of the average contour length of micelles L upon absorption of hydrocarbon. Indeed, for a Maxwell fluid the relaxation time should depend on L as $\tau = (\tau_{\text{rep}}\tau_{\text{br}})^{1/2} \sim L$ by taking into account the scaling dependences of the reptation time $\tau_{\text{rep}} \sim L^3$ and breaking time $\tau_{\text{br}} \sim L^{-1}$ on the average contour length L .⁴⁷

Thus, shortening of the micelles seems to be responsible for the decreases in both G_0 and τ . The reasons for the shortening of the micellar chains upon absorption of hydrocarbon can be easily understood from the microscopic point of view. We know that the average length of a cylindrical micelle is controlled by the end-cap energy (scission energy) δ given by eq 7, which reflects the fact that the molecules in the end caps are not optimally packed. (Indeed, if they were able to pack ideally into a sphere, they would have formed spherical instead of wormlike micelles). If the absorption of hydrocarbon molecules into the cylindrical micelle can reduce the scission energy δ , then wormlike micelles will become shorter. It is easy to see that this is indeed the case. The scission energy δ originates from the fact that in the semispherical end cap each molecule is confined within a volume of conical shape, which leads to a nonoptimal surface area per molecule head (Theoretical Section). Now, if a hydrocarbon droplet is added to the center of the end cap, the end cap swells and

the volume accessible to one surfactant molecule changes its shape from a cone to a truncated cone. Because both the total volume of the molecule and its length are fixed, the outer surface area per surfactant molecule decreases with this change in shape and becomes closer to the optimal value. (In turn, the inner surface that corresponds to the interface between surfactant tails and hydrocarbon increases, but we assume that there is no surface tension associated with this interface because of their similar chemical natures.) This leads to the reduction of the scission energy 2δ and, therefore, according to eq 8, a reduction of the average length of the micelles.

The more quantitative description of this effect is developed in the Supporting Information, with the main result being given by eq 11. As hydrocarbon is added, the scission energy is reduced and reaches zero (assuming that hydrocarbon is absorbed only in the end caps) at some critical hydrocarbon concentration c_h^{crit} . This critical concentration depends on the concentration of the amphiphiles c and on their chemical structure (in particular, on how strongly the end caps are strained in the first place). Overall, one can estimate that

$$c_h^{\text{crit}} \leq c \frac{(r_{\text{min}} - b)^3}{r_{\text{min}}^3 - (r_{\text{min}} - b)^3} \approx \frac{c}{19} \quad (11)$$

$$r_{\text{min}} = b \left(1 + \frac{1}{\sqrt{3}} \right) \quad (12)$$

where r_{min} is the minimum possible radius of a droplet.

This result for the critical concentration is somewhat smaller than that suggested by the experimental data presented above (Figure 1). This discrepancy can be explained as follows. The theoretical prediction of eq 11 is based on the assumption that hydrocarbon will fill only the end caps. However, the hydrocarbon molecules can, in principle, absorb both in the end caps and in the cylindrical body of the micelles. Absorption in the end caps is energetically preferable because it allows the relaxation of the existing strain of the surfactants in the end caps, but because the micelles are very long, absorption into the larger volume of the cylindrical body is entropically favored. (There are many more places in the body of the micelles than in the end caps.)

From Figure 1 it is seen that the transition point from the first to the second regime for 3 wt % surfactant corresponds to 0.18 wt % ≈ 10 mM added hydrocarbon. However, the theoretical critical concentration of hydrocarbon in this case is $c/19 = 5$ mM. Thus, in comparing the experimental data and theoretical expectation, we estimate that at the transition point approximately half of the hydrocarbon molecules are absorbed in the end caps and half are absorbed in the cylindrical body of the micelles. Because the average length of the micelles at the transition point is on the order of 1000 Å (calculated from eqs 9 and 10 using the approximate value $l_p = 188$ Å taken from Table 1), it can be estimated that the total volume of surfactant molecules forming the cylindrical body is 10–40 times higher than the total volume of surfactant forming the end caps. (The volume of surfactant in the end caps increases as the microdroplets of the hydrocarbon are formed inside.) Thus, the number of hydrocarbon molecules per surfactant molecule in the cylindrical body is lower than in the end caps by at least 1 order of magnitude (i.e., the end caps absorb hydrocarbon much more effectively). It should be noted that this is the first semiquantitative attempt to estimate the distribution of

hydrocarbon between the cylindrical body and spherical end caps of wormlike micelles.

Thus, the slight decrease in viscosity upon addition of hydrocarbon observed in region I is attributed to the shortening of the entangled micellar chains, which takes place as a result of the absorption of hydrocarbon preferentially in the end caps, thus making the end caps more energetically favorable.

Transition Regime. In this regime, the viscosity of the solution decreases sharply upon addition of small amounts of hydrocarbon (Figure 1). For instance, for 3 wt % potassium oleate solutions the viscosity drops by 4 orders of magnitude as the concentration of *n*-dodecane increases from 0.15 to 0.5 wt %. Simultaneously, the system starts to deviate strongly from the Maxwell model (Figure 2b). The greater the amount of added hydrocarbon, the more pronounced the deviation. This deviation is likely due to the progressive shortening of the micellar chains. Indeed, when the micellar length diminishes, the reptation time τ_{rep} decreases and the breaking time τ_{br} becomes larger (because for a shorter micelle there are fewer points where it can be broken). As a result, the system moves away from the fast-breaking limit ($\tau_{\text{br}} \ll \tau_{\text{rep}}$) and approaches the limit of so-called “dead” micelles, which do not break and recombine during reptation ($\tau_{\text{br}} > \tau_{\text{rep}}$) and therefore do not obey simple Maxwell behavior.²³ Indeed, in the vicinity of the transition point from the first to the second regime (i.e., at fixed molar ratio [hydrocarbon]/[surfactant] = 1/11 for 3 wt % potassium oleate) the scaling dependence of viscosity η_0 on surfactant concentration (Figure 6) reflects the behavior inherent to “dead” micelles:⁴⁷ $\eta_0 \sim c^{5.25}$ (compared to what is seen in the first regime: $\eta_0 \sim c^{3.5}$ (Figure 3)).

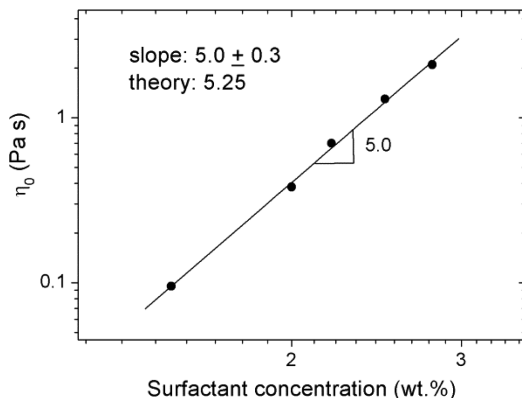


Figure 6. Dependence of zero-shear viscosity on potassium oleate concentration at a fixed molar ratio [n-dodecane]/[potassium oleate] = 1/11. Temperature: 20 °C. Solvent: 6 wt % KCl in water.

According to Figure 5, at hydrocarbon concentrations close to the transition between the first and the second regimes (ca. 0.15 wt %) the average length of micellar chains L approaches l_e so that the reptation mechanism no longer reflects the relaxation process in the system. Therefore, a sharp drop in viscosity correlates with the crossover from entangled to unentangled behavior of the wormlike micellar solution taking place upon shortening of micellar chains.

However, the decrease in viscosity observed in the second regime is too steep to be explained only by the decrease in the micelle length. Indeed, as estimated above, at the beginning of this regime L is ca. 1000 Å, but the value of L should decrease by over 4 orders of magnitude to account for the observed decrease in viscosity ($\eta \sim L$ for the unentangled regime⁵⁰),

which is unrealistic. To explain this discrepancy, one can suggest that in region II microemulsion droplets already start to form and contribute to the decrease in viscosity because they compete with the wormlike micelles for surfactant molecules.

To check this hypothesis, SANS was used. Typical scattering curves obtained are presented in Figure 7. It was shown that at

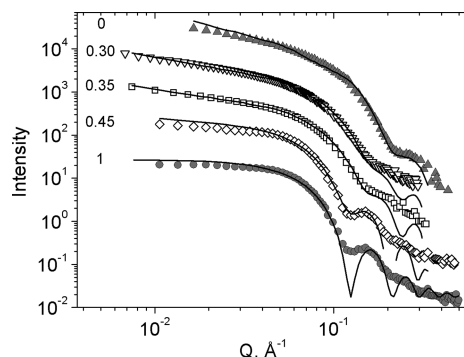


Figure 7. SANS profiles for 3 wt % potassium oleate solutions in the presence of different concentrations of *n*-dodecane as indicated (in wt %). The data for 1 wt % *n*-dodecane are absolute values, and the other curves are offset by factors of 7, 50, 250, and 2000 for a better representation. Solid lines represent the fits by form factors of a cylinder (0 wt % *n*-dodecane), of a mixture of cylinders and spheres (0.30, 0.35, and 0.45 wt % *n*-dodecane), and of a sphere (1 wt % *n*-dodecane). Temperature: 20 °C. Solvent: 6 wt % KCl in D₂O.

0.3, 0.35, and 0.45 wt % *n*-dodecane the SANS curves can be described neither by a pure cylinder form factor (which works well in the first regime) nor by the sphere form factor (which works in the third regime). The best fits of the curves can be obtained by using a sum of cylinder and sphere form factors (Figure 7). The results of fitting are summarized in Table 2. As is seen, at increasing hydrocarbon concentration the volume fraction and radius of the droplets increase while the volume fraction of cylindrical micelles becomes smaller. Note that the minimum radius of spherical droplets observed (Table 2) is consistent with the value (30 Å) predicted theoretically by eq 12 and is larger than the length of a fully extended surfactant tail (19 Å). Also, it can be seen that the radius of the cylinder changes insignificantly upon addition of hydrocarbon and is close to the length of the fully stretched surfactant tail.

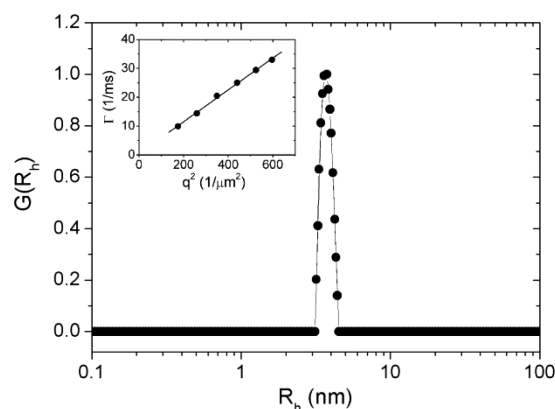
Thus, SANS data provide evidence for the coexistence of cylindrical micelles and microemulsion droplets within the transition region. To the best of our knowledge, this is the first observation of such coexistence made by SANS. Previously, such coexistence was observed by cryo-TEM for nonionic surfactant pentaethylene glycol monododecyl ether C₁₂E₅ in the presence of *n*-octane, but with much larger amounts of added hydrocarbon.⁵¹

Therefore, in the transition regime (region II) wormlike micelles are short and unentangled, and the viscosity of the system decreases by several orders of magnitude as a result of both the decreasing length of wormlike micelles and the appearance of microemulsion droplets that do not significantly contribute to the viscosity.

Microemulsion Regime. In the microemulsion regime, the viscosity remains constant at the pure water value (Figure 1). SANS curves of the solutions in this regime (Figure 7) are well fit by the form factor of a sphere with a radius of 38 Å, indicating the presence of only microemulsion droplets in the solution. This result is consistent with DLS data (Figure 8).

Table 2. Results of Fitting the SANS Data by Form Factors of a Cylinder, a Sphere, or a Mixture of Cylinders and Spheres for 3 wt % Potassium Oleate Solutions in the Presence of Different Concentrations of *n*-Dodecane

concentration of <i>n</i> -dodecane, wt %	volume fraction of cylinders	volume fraction of spheres (microemulsion droplets)	radius of cylinder, Å	radius of sphere (microemulsion droplet), Å
0	1	0	18.3 ± 0.3	
0.30	0.53 ± 0.05	0.47 ± 0.05	19.5 ± 0.2	31.6 ± 0.4
0.35	0.40 ± 0.05	0.60 ± 0.05	19.2 ± 0.3	32.0 ± 0.5
0.45	0.25 ± 0.05	0.75 ± 0.05	19.3 ± 0.3	37.5 ± 0.2
1	0	1	-	37.9 ± 0.2

**Figure 8.** Distribution function of hydrodynamic radii obtained by the Contin method at scattering angle $\theta = 90^\circ$ (relaxation rate Γ as a function of the square of the scattering vector q^2 in the inset) for a 3 wt % potassium oleate solution in the presence of 1 wt % *n*-dodecane. Temperature: 20 °C. Solvent: 6 wt % KCl in water.

DLS measurements show that in this regime the correlation functions are monomodal with the relaxation rate Γ being directly proportional to the square of the scattering vector q^2 (Figure 8, inset), which demonstrates that this mode is due to the translational diffusion of particles (i.e., microemulsion droplets). The distribution of hydrodynamic radii of the droplets is rather narrow and has a maximum at 38 Å (Figure 8). Thus, the radius of microemulsion droplets is 2-fold larger than the length of a fully extended alkyl tail of potassium oleate (19 Å), indicating that the droplets consist of a hydrocarbon core with a radius of 19 Å surrounded by one layer of surfactant molecules with a thickness of 19 Å. This corresponds to roughly 76 molecules of *n*-dodecane and 420 molecules of potassium oleate per droplet assuming that all of the core is filled with hydrocarbon and all of the shell is composed of surfactant. But it should be noted that at the transition point from the second to the third regime (0.5 wt % *n*-dodecane for a 3 wt % potassium oleate solution) the volume ratio of surfactant to hydrocarbon is ~ 4.7 whereas the volume ratio of the spherical shell (radius 38 Å, thickness 19 Å) to the inner sphere (radius 19 Å) is equal to 7.0. This interesting fact indicates that there is some penetration of hydrocarbon molecules into the volume of the spherical shell occupied by surfactant tails. A similar conclusion was made in ref 26 for a tetradecyltrimethylammonium bromide/sodium salicylate system with added short-chain hydrocarbons (hexane and octane).

Note that only 0.5 wt % *n*-dodecane, which corresponds to one hydrocarbon molecule per three surfactant molecules, is necessary to transform nearly all wormlike micelles into microemulsion droplets for a 3 wt % surfactant solution. For a 2-fold decrease in the potassium oleate concentration, this

critical amount of *n*-dodecane decreases by a factor of 2.5 (Figure 1). Thus, very small amounts of hydrocarbon induce dramatic changes in the rheology and structure of wormlike micelles, which are transformed into microemulsion droplets. Moreover, the results obtained in this study open the way to further reductions in the amount of oil required to induce a pronounced decrease in viscosity. One such way may consist of taking the viscoelastic solution of surfactant just in the vicinity of the transition from the entangled to the unentangled regime.

CONCLUSIONS

In this article, the whole range of transition of wormlike surfactant micelles to microemulsion droplets upon addition of small amounts of hydrocarbon was investigated. For this purpose, several complementary techniques were used: rheology to study macroscopic properties (viscosity, elasticity, etc.) and scattering techniques (SANS and DLS) to follow the structural changes occurring on the microscopic level. Our rheological data show that the transition of wormlike micelles to microemulsion droplets can be subdivided into three regions: (i) region I, where the solutions retain high viscosity (~ 10 – 350 Pa·s); (ii) region II, where the solution viscosity sharply decreases by 4 orders of magnitude; and (iii) region III, where the viscosity is close to that of pure water (~ 0.001 Pa·s). Our theoretical analysis of hydrocarbon absorption by the surfactant micelles in region I suggests that the preferential mechanism of hydrocarbon encapsulation is its accumulation in the energetically unfavorable end caps of wormlike micelles, which reduces the micelle scission energy and leads to the shortening of the micellar chains. This conclusion is consistent with experimental results that indicate that wormlike micelles are entangled but their length is reduced by the solubilization of hydrocarbon. When wormlike micelles become sufficiently short, a transition to the unentangled micelle regime occurs, which coincides with the crossover from region I to region II. In the second region, further micelle shortening proceeds simultaneously with the formation of microemulsion droplets. The coexistence of cylindrical wormlike micelles and spherical microemulsion droplets is evidenced by the SANS data analysis. Because microemulsion droplets do not significantly contribute to the viscosity, an increase in their fraction with the addition of hydrocarbon results in a dramatic decrease in the viscosity observed in this region. In region III, only microemulsion droplets remain in the system, resulting in a low viscosity of solution. SANS and DLS data indicate that microemulsion droplets are rather monodisperse with a characteristic size of 38 Å. Thus, as a result of these studies it is demonstrated that a small amount of hydrocarbon induces a dramatic drop in the viscosity of the system, which is due to the shortening of micellar chains with the concurrent formation of microemulsion droplets. The obtained structural details of the wormlike micelle to microemulsion transformation and the

proposed molecular mechanism are of obvious importance to the development of new highly responsive systems based on wormlike surfactant micelles, which can be used, in particular, as one of the main components in fracturing fluids for enhanced oil recovery, where the responsiveness to hydrocarbons is a key property.

■ ASSOCIATED CONTENT

■ Supporting Information

Determination of the persistence length of cylindrical micelles l_p from SANS data and theoretical estimation of the scission energy of a cylindrical micelle with solubilized hydrocarbon. This material is available free of charge via the Internet at <http://pubs.acs.org>.

■ AUTHOR INFORMATION

Corresponding Author

*Fax: +7 495 9392988. Tel: +7 495 9391464. E-mail: phil@poly.phys.msu.ru.

Notes

The authors declare no competing financial interest.

■ ACKNOWLEDGMENTS

This work was supported by the Russian Foundation for Basic Research. A.V.S. gratefully acknowledges LG Chem for a scholarship. We express our gratitude to Prof. A. N. Semenov for fruitful discussions.

■ REFERENCES

- (1) Dreiss, C. A. Wormlike Micelles, Where Do We Stand? Recent Development, Linear Rheology and Scattering Techniques. *Soft Matter* **2007**, *3*, 956–970.
- (2) Raghavan, S. R.; Kaler, E. W. Highly Viscoelastic Wormlike Micellar Solutions Formed by Cationic Surfactants with Long Unsaturated Tails. *Langmuir* **2001**, *17*, 300–306.
- (3) Kumar, R.; Kalur, G. C.; Ziserman, L.; Danino, D.; Raghavan, S. R. Wormlike Micelles of a C22-Tailed Zwitterionic Surfactant: From Viscoelastic Solutions to Elastic Gels. *Langmuir* **2007**, *23*, 12849–12856.
- (4) Hoffmann, H. In *Structure and Flow in Surfactant Solutions*; Herb, C. A., Prud'homme, R. K., Eds.; ACS Symposium Series 578; American Chemical Society: Washington, DC, 1994.
- (5) Cates, M. E. Reptation of Living Polymers: Dynamics of Entangled Polymers in the Presence of Reversible Chain-Scission Reactions. *Macromolecules* **1987**, *20*, 2289–2296.
- (6) Cates, M. E.; Candau, S. J. Statics and Dynamics of Wormlike Surfactant Micelles. *J. Phys.: Condens. Matter* **1990**, *2*, 6869–6892.
- (7) Granek, R.; Cates, M. E. Stress Relaxation in Living Polymers: Results from a Poisson Renewal Model. *J. Chem. Phys.* **1992**, *96*, 4758–4767.
- (8) Rose, G. D.; Foster, K. L. Drag Reduction and Rheological Properties of Cationic Viscoelastic Surfactant Formulations. *J. Non-Newtonian Fluid Mech.* **1989**, *31*, 59–85.
- (9) Chase, B.; Chmiliowski, W.; Marcinew, R.; Mitchell, C.; Dang, Y.; Krauss, D.; Nelson, E.; Lantz, T.; Parham, C.; Plummer, J. Clear Fracturing Fluids for Increased Well Productivity. *Oilfield Rev.* **1997**, *9*, 20–33.
- (10) Maitland, G. C. The Colloid and Interface Science of Oil and Gas Production. *Curr. Opin. Colloid Interface Sci.* **2000**, *5*, 301–311.
- (11) Kefi, S.; Lee, J.; Pope, T. L.; Sullivan, P.; Nelson, E.; Hernandez, A. N.; Olsen, T.; Parlar, M.; Powers, B.; Roy, A.; Wilson, A.; Twynam, A. Expanding Applications for Viscoelastic Surfactants. *Oilfield Rev.* **2004/2005**, *16*, 10–23.
- (12) Törnblom, M.; Henriksson, U. Effect of Solubilization of Aliphatic Hydrocarbons on Size and Shape of Rodlike C16TABr

Micelles Studied by ^2H NMR Relaxation. *J. Phys. Chem. B* **1997**, *101*, 6028–6035.

(13) Kumar, S.; Bansal, D.; Kabir-ud-Din. Micellar Growth in the Presence of Salts and Aromatic Hydrocarbons: Influence of the Nature of the Salt. *Langmuir* **1999**, *15*, 4960–4965.

(14) Siriawatwechakul, W.; LaFleur, T.; Prud'homme, R. K.; Sullivan, P. Effects of Organic Solvents on the Scission Energy of Rodlike Micelles. *Langmuir* **2004**, *20*, 8970–8974.

(15) Rogriguez-Abreu, C.; Aramaki, K.; Tanaka, Y.; Lopez-Quintela, A.; Ishitobi, M.; Kunieda, H. Wormlike Micelles and Microemulsions in Aqueous Mixtures of Sucrose Esters and Nonionic Cosurfactants. *J. Colloid Interface Sci.* **2005**, *291*, 560–569.

(16) Sato, T.; Acharya, D. P.; Kaneko, M.; Aramaki, K.; Singh, Y.; Ishitobi, M.; Kunieda, H. Oil-Induced Structural Change of Wormlike Micelles in Sugar Surfactant Systems. *J. Dispersion Sci. Technol.* **2006**, *27*, 611–616.

(17) Sharma, S. C.; Acharya, D. P.; Aramaki, K. Viscoelastic Micellar Solutions in a Mixed Nonionic Fluorinated Surfactants System and the Effect of Oils. *Langmuir* **2007**, *23*, 5324–5330.

(18) Miyake, M.; Asano, A.; Einaga, Y. Size Change of the Wormlike Micelles of Pentaerythritol, Hexaerythritol, and Heptaerythritol Dodecyl Ethers with Uptake of *n*-Dodecane. *J. Phys. Chem. B* **2008**, *112*, 4648–4655.

(19) Afifi, H.; Karlsson, G.; Heenan, H.; Dreiss, C. A. Solubilization of Oils or Addition of Monoglycerides Drives the Formation of Wormlike Micelles with an Elliptical Cross-Section in Cholesterol-Based Surfactants: A Study by Rheology, SANS, and Cryo-TEM. *Langmuir* **2011**, *27*, 7480–7492.

(20) Mukerjee, P.; Cardinal, J. R. Benzene Derivatives and Naphthalene Solubilized in Micelles. Polarity of Microenvironments, Location and Distribution in Micelles, and Correlation with Surface Activity in Hydrocarbon-Water Systems. *J. Phys. Chem.* **1978**, *82*, 1620–1627.

(21) Menge, U.; Lang, P.; Findenegg, G. H. Structural Transition of Oil-Swollen Cylindrical Micelles of C_{12}E_5 in Water Studied by SANS. *J. Phys. Chem. B* **2003**, *107*, 1316–1320.

(22) Hoffmann, H.; Würtz, J. Unusual Phenomena in Perfluorosurfactants. *J. Mol. Liq.* **1997**, *72*, 191–230.

(23) Shashkina, J. A.; Philippova, O. E.; Zaruslov, Yu. D.; Khokhlov, A. R.; Pryakhina, T. A.; Blagodatskikh, I. V. Rheology of Viscoelastic Solutions of Cationic Surfactant. Effect of Added Associating Polymer. *Langmuir* **2005**, *21*, 1524–1530.

(24) Molchanov, V. S.; Philippova, O. E.; Khokhlov, A. R.; Kovalev, Yu. A.; Kuklin, A. I. Self-Assembled Networks Highly Responsive to Hydrocarbons. *Langmuir* **2007**, *23*, 105–111.

(25) Philippova, O. E.; Molchanov, V. S. Polymer-Surfactant Networks Highly Responsive to Hydrocarbons. *Macromol. Symp.* **2010**, *291–292*, 137–143.

(26) Hoffmann, H.; Ulbrich, W. Transition of Rodlike to Globular Micelles by the Solubilization of Additives. *J. Colloid Interface Sci.* **1989**, *129*, 388–405.

(27) See, for example, May, S.; Ben-Shaul, A. In *Giant Micelles: Properties and Applications*; Zana, R., Kaler, E., Eds.; CRC Press: Boca Raton, FL, 2007 and references therein.

(28) Wittmer, J. P.; Milchev, A.; Cates, M. E. Dynamical Monte Carlo Study of Equilibrium Polymers: Static Properties. *J. Chem. Phys.* **1998**, *109*, 834–845.

(29) Padding, J. T.; Boek, E. S.; Briels, W. J. Dynamics and Rheology of Wormlike Micelles Emerging from Particulate Computer Simulations. *J. Chem. Phys.* **2008**, *129*, 074903-1–074903-11.

(30) Nagarajan, R.; Ruckenstein, E. Theory of Surfactant Self-Assembly: A Predictive Molecular Thermodynamics Approach. *Langmuir* **1991**, *7*, 2934–2969.

(31) Nagarajan, R. Solubilization by Amphiphilic Aggregates. *Curr. Opin. Colloid Interface Sci.* **1997**, *2*, 282–293.

(32) Karaborni, S.; van Os, N. M.; Esselink, K.; Hilbers, P. A. J. Molecular Dynamics Simulations of Oil Solubilization in Surfactant Solutions. *Langmuir* **1993**, *9*, 1175–1178.

- (33) Reiss-Husson, F.; Luzatti, V. The Structure of the Micellar Solutions of Some Amphiphilic Compounds in Pure Water as Determined by Absolute Small-Angle X-Ray Scattering Techniques. *J. Phys. Chem.* **1964**, *68*, 3504–3511.
- (34) Fukuda, H.; Goto, A.; Yoshioka, H.; Goto, R.; Morigaki, K.; Walde, P. An Electron Spin Resonance Study of the pH-Induced Transformation of Micelles to Vesicles in an Aqueous Oleic Acid/Oleate System. *Langmuir* **2001**, *17*, 4223–4231.
- (35) Zaruslov, Yu. D.; Gordeliy, V. I.; Kuklin, A. I.; Islamov, A. H.; Philippova, O. E.; Khokhlov, A. R.; Wegner, G. Self-Assembly of Polyelectrolyte Rods in Polymer Gel and in Solution: Small-Angle Neutron Scattering Study. *Macromolecules* **2002**, *35*, 4466–4471.
- (36) Philippova, O. E.; Andreeva, A. S.; Khokhlov, A. R.; Islamov, A. K.; Kuklin, A. I.; Gordeliy, V. I. Charge-Induced Microphase Separation in Polyelectrolyte Hydrogels with Associating Hydrophobic Side Chains: Small-Angle Neutron Scattering Study. *Langmuir* **2003**, *19*, 7240–7248.
- (37) Andreeva, A. S.; Philippova, O. E.; Khokhlov, A. R.; Islamov, A. K.; Kuklin, A. I. Effect of the Mobility of Charged Units on the Microphase Separation in Amphiphilic Polyelectrolyte Hydrogels. *Langmuir* **2005**, *21*, 1216–1222.
- (38) Soloviev, A. G.; Stadnik, A. V.; Islamov, A. K.; Kuklin, A. I. FITTER: The Package for Fitting Experimental Data of the YuMO Spectrometer by Theoretical Form Factors. Version 1.0. Long Write-Up and User's Guide. *Commun. Jt. Inst. Nucl. Res., Dubna* **2003**, E10-2003-36.
- (39) Konarev, P. V.; Volkov, V. V.; Sokolova, A. V.; Koch, M. H. J.; Svergun, D. I. PRIMUS: a Windows PC-based System for Small-Angle Scattering Data Analysis. *J. Appl. Crystallogr.* **2003**, *36*, 1277–1282.
- (40) Korchagina, E. V.; Philippova, O. E. Multichain Aggregates in Dilute Solutions of Associating Polyelectrolyte Keeping a Constant Size at the Increase in the Chain Length of Individual Macromolecules. *Biomacromolecules* **2010**, *11*, 3457–3466.
- (41) Philippova, O. E.; Korchagina, E. V.; Volkov, E. V.; Smirnov, V. A.; Khokhlov, A. R.; Rinaudo, M. Aggregation of Some Water-Soluble Derivatives of Chitin in Aqueous Solutions: Role of the Degree of Acetylation and Effect of Hydrogen Bond Breaker. *Carbohydr. Polym.* **2012**, *87*, 687–694.
- (42) Korchagina, E. V.; Philippova, O. E. Effects of Hydrophobic Substituents and Salt on Core–Shell Aggregates of Hydrophobically Modified Chitosan: Light Scattering Study. *Langmuir* **2012**, *28*, 7880–7888.
- (43) Israelachvili, J. N. *Intermolecular and Surface Forces*, 2nd ed.; Academic Press: London, 1992.
- (44) Molchanov, V. S.; Shashkina, Y. A.; Philippova, O. E.; Khokhlov, A. R. Viscoelastic Properties of Aqueous Anionic Surfactant (Potassium Oleate) Solutions. *Colloid J.* **2005**, *67*, 606–609.
- (45) Flood, C.; Dreiss, C. A.; Croce, V.; Cosgrove, T.; Karlsson, G. Wormlike Micelles Mediated by Polyelectrolyte. *Langmuir* **2005**, *21*, 7646–7652.
- (46) Rehage, H.; Hoffmann, H. Viscoelastic Surfactant Solutions: Model Systems for Rheological Research. *Mol. Phys.* **1991**, *74*, 933–973.
- (47) Magid, L. J. The Surfactant-Polyelectrolyte Analogy. *J. Phys. Chem. B* **1998**, *102*, 4064–4074.
- (48) Pimenta, P.; Pashkovsky, E. E. Rheology of Viscoelastic Mixed Surfactant Solutions: Effect of Scission on Nonlinear Flow and Rheochaos. *Langmuir* **2006**, *22*, 3980–3987.
- (49) Bayer, O.; Hoffmann, H.; Ulbrich, W.; Thurn, H. The Influence of Solubilized Additives on Surfactant Solutions with Rodlike Micelles. *Adv. Colloid Interface Sci.* **1986**, *26*, 177–203.
- (50) Larson, R. G. *The Structure and Rheology of Complex Fluids*; Oxford University Press: New York, 1999; p 108.
- (51) Bernheim-Grosswasser, A.; Tlustý, T.; Safran, S. A.; Talmon, Y. Direct Observation of Phase Separation in Microemulsion Networks. *Langmuir* **1999**, *15*, 5448–5453.